A Kinetics and Mechanistic Study of the Atmospherically Relevant Reaction between Molecular Chlorine and Dimethyl Sulfide (DMS)

by

J.M.Dyke[(a)]*, M.V.Ghosh [(a)] , D.J.Kinnison [(a)] , G.Levita[(a)] , A. Morris[(a)] and D.E.Shallcross [(b)]

(a) School of Chemistry, University of Southampton, Southampton SO17 1BJ, UK

(b) Bristol Biogeochemistry Research Centre, School of Chemistry, University of Bristol, Bristol, BS8 1TS, UK

* to whom correspondence should be addressed

Contribution to a Special Issue of PCCP in honour of Prof.V.E.Bondybey

Abstract

A gas-phase kinetics study of the atmospherically important reaction between Cl_2 and dimethyl sulfide (DMS)

$$Cl_2 + CH_3SCH_3 \rightarrow \text{products} \quad \text{-----} \quad (1)$$

has been made using a flow-tube interfaced to a photoelectron spectrometer. The rate constant for this reaction has been measured at 1.6 and 3.0 torr at T= (294±2) K as (3.4 ± 0.7) x 10^{-14} cm^3 $molecule^{-1}s^{-1}$. Reaction (1) has been found to proceed via an intermediate, $(CH_3)_2SCl_2$, to give CH_3SCH_2Cl and HCl as the products.

The mechanism of this reaction and the structure of the intermediate were investigated using electronic structure calculations. A comparison of the mechanisms of the reactions between Cl atoms and DMS, and Cl_2 and DMS has been made and the relevance of the results to atmospheric chemistry is discussed.

Introduction

This paper reports the first study in which a flow-tube has been interfaced to a photoelectron spectrometer to allow a gas-phase kinetics study to be performed on an atmospherically important reaction. Ultraviolet photoelectron spectroscopy (PES) has the advantage over mass spectrometry in that it does not suffer from fragmentation problems. It has the potential to observe reactants, intermediates and products and to measure branching ratios between reaction channels which give different intermediates and/or final products. An example of a reaction studied by PES in Southampton in which different intermediates were observed is the reaction between F atoms and propane which gives rise to the n-propyl and iso-propyl radicals as primary products (1). The only previous use of PES in a kinetics study is the work of Wang et al., who studied the unimolecular thermal rearrangements of a number of compounds (2-4), notably isomerisation of CH_3NC to CH_3CN (2) and isomerisation of SSF_2 to FSSF (3).

The reaction studied in this work is the atmospherically important reaction between molecular chlorine and dimethyl sulfide (DMS)

$$Cl_2 + CH_3SCH_3 \rightarrow \text{products} \qquad \text{-----} \quad (1)$$

This work, as well as related research with photoelectron, infrared and ultraviolet/visible spectroscopy and *ab initio* molecular orbital calculations (5), has shown that this reaction proceeds *via* a covalently bound intermediate, $(CH_3)_2SCl_2$, and to give CH_3SCH_2Cl and HCl as the products.

The sulfur cycle in the earth's atmosphere has been the subject of intensive investigation in recent years because of the need to assess the contribution of anthropogenically produced sulfur to acid rain, visibility reduction and climate modification. Anthropogenic emissions of sulfur to the atmosphere are dominated by SO_2 whereas natural (biogenic) sulfur emissions are thought to be dominated by dimethyl sulfide derived from oceanic phytoplankton (6-9). At present, anthropogenic emissions of sulfur dominate; however, these emissions are predominantly in the northern hemisphere. In the southern hemisphere and in particular the southern oceans, natural emissions are extremely important. The primary step of DMS oxidation in the atmosphere is predominantly reaction with the OH radical during the day and the NO_3 radical at night. Subsequent oxidation in the atmosphere leads to formation of species such as SO_2, H_2SO_4 and CH_3SO_3H (methane sulfonic acid or MSA). These species may contribute significantly to the acidity of the atmosphere and in the case of sulphuric acid to cloud formation (9).

Recently molecular chlorine has been observed in coastal marine air. This is produced at night, as well as during the day, from heterogeneous reactions of ozone with wet sea-salt and is enhanced by the presence of ferric ions (10). Employing a high-pressure chemical ionization mass spectrometry technique, Spicer *et al*. (11) measured Cl_2 levels ranging from <15 to 150 pptv. Night-time Cl_2 mixing ratios were in the range 40-150 pptv, with the highest value being observed near mid-night, which dropped to 15 pptv in day-light. A modelling study conducted in this work found that, shortly after sunrise, the oxidation rate of DMS by Cl, produced by photolysis of Cl_2, could under favourable conditions, be an order of magnitude higher than the rate of oxidation by OH. The rate constant for the reaction between Cl atoms and DMS at 298 K and 1 torr pressure has been measured as $(6.9 \pm 1.3) \times 10^{-11}$ cm^3 molecule^{-1}s^{-1} using discharge-flow mass spectrometry (12), and at 3 torr pressure and at 297 K it has been measured as $(1.8 \pm 0.3) \times 10^{-10}$ cm^3 molecule^{-1}s^{-1} using time-resolved resonance detection of Cl (13). A more recent study using cavity ring-down spectroscopy (14) determined the rate constant at atmospheric pressure as $(3.6 \pm 0.2) \times 10^{-10}$ cm^3 molecule^{-1}s^{-1} and a low-pressure limit rate constant consistent with that found in references (12) and (13). It has been found that the Cl + DMS reaction, reaction (2),

proceeds *via* two routes, a direct stripping channel (2a) that proceeds without a barrier to give CH_3SCH_2 and HCl and an addition channel (2b) to give $(CH_3)_2SCl$ (13-16).

$$Cl + CH_3SCH_3 \rightarrow CH_3SCH_2 + HCl \quad \text{--------} \quad (2a)$$

$$Cl + CH_3SCH_3 + M \rightarrow (CH_3)_2SCl + M \quad \text{--------} \quad (2b)$$

$$(CH_3)_2SCl \rightarrow CH_3 + CH_3SCl \quad \text{--------} \quad (2c)$$

Decomposition of the adduct to produce CH_3SCl and CH_3 (reaction 2c) is very slow, as it has a high activation energy barrier, and is not competitive with CH_3SCH_2 and HCl production (16).
Given the known presence of both DMS and Cl_2 in the marine boundary layer, it was thought valuable to measure the rate constant of reaction (1) at room temperature and determine its products, using a recently developed instrument which interfaces a flow-tube to a u.v. photoelectron spectrometer *via* several stages of differential pumping. In addition, to complement the experimental work, molecular orbital calculations were used to determine relative energies of intermediates and their decomposition products, and study the mechanism of reaction (1). The rate constant of this reaction has not been measured previously, although a discharge-flow electron impact mass spectrometric study (17) gave an upper limit for the rate constant of 8×10^{-14} cm^3 $molecule^{-1}s^{-1}$.

Experimental Details

The apparatus used to study reaction (1) consists of a stainless steel flow-tube connected via a differential pumping system to a photoelectron spectrometer designed to study short-lived species in the gas-phase. All experiments were performed at total pressures of 1.6 and 3.0 torr and at room temperature (294±2) K. Helium was used as the carrier gas in all experiments.
Figure 1 is a block diagram of the central part of the apparatus.

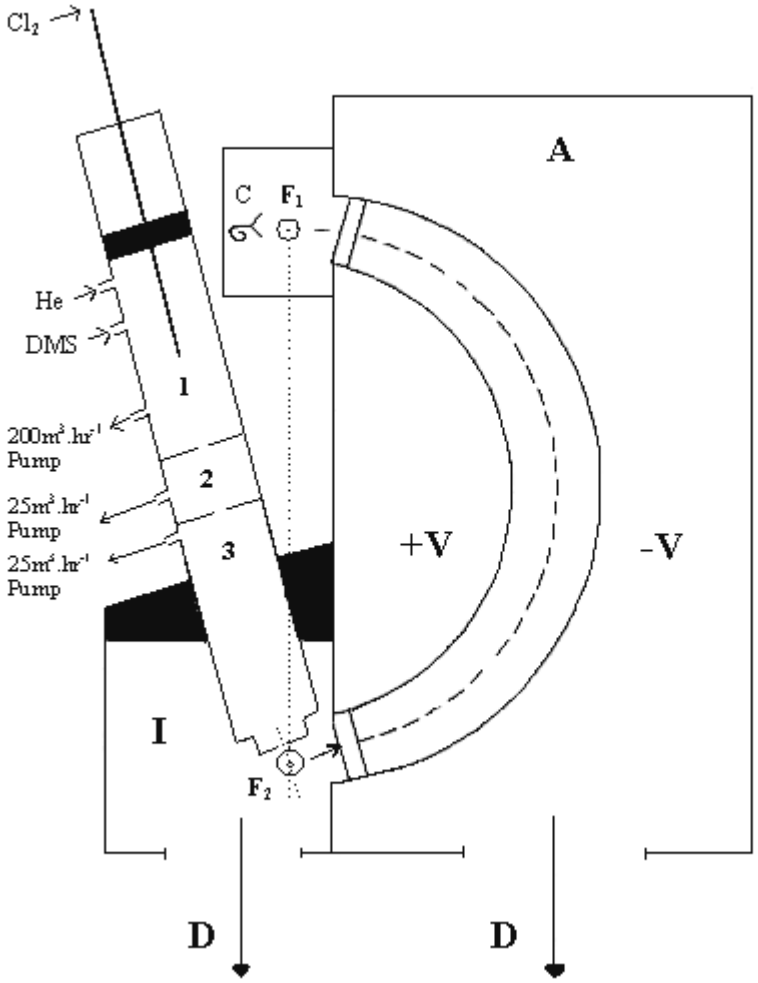

Figure1: Schematic diagram of the flow-tube used in this work, using detection with a photoelectron spectrometer

In this figure:-
A-Analyser Chamber, I-Ionization Chamber, C-Channeltron,
D-diffusion pump, ±V Hemisphere Voltages, F1-exit focus,
F2-entrance focus, 1- Chamber 1 of flow-tube (total pressure ~3 torr),
2,3-Chamber 2 and 3 of the differential pumping system (approximate pressures ~10^{-1} torr, ≤ 10^{-2} torr respectively).

Figure 1 shows the flow-tube positioned at an angle of 15^{o} to the vertical, attached to the ionization chamber of the photoelectron spectrometer and aligned perpendicular to the photon source.

The flow-tube

The flow-tube used consists of a 50 cm long stainless steel tube with an inner diameter of 3 cm. It was pumped by a SV 200 pump (Leybold) that provides linear flow velocities from 3 ms^{-1} up to 40 ms^{-1} of the carrier gas (helium). The total gas pressure in the flow-tube was measured downstream by a capacitance manometer (MKS Baratron, 10 torr range). In this study the pressure within the flow reactor was changed between 1.6 and 3.0 torr and linear flow velocities between 3 and 8 ms^{-1} were employed. The character of the flow in the flow-tube was laminar, as calculated Reynolds numbers were below 2000. Under these conditions the flow is characterised by a parabolic velocity profile across the flow-tube; the molecules close to the walls experience a higher viscous drag than those in the middle of the flow-tube and so have a lower velocity.

The kinetics experiments presented in this work were performed under pseudo-first-order conditions. Chlorine, the reactant in excess (10^{14}-10^{15} molecules cm^{-3}), was added through the movable injector (70 cm long) and DMS (concentrations less than 10^{13} molecules cm^{-3}) entered the flow tube through the fixed side arm. Contact times were between 20 and 150 ms. The pseudo-first-order rate constant was determined by measuring the relative concentration of DMS, from the intensity of its first photoelectron band, with the movable injector at several different positions while the chlorine partial pressure was in excess and held constant (18). This was then repeated at different chlorine partial pressures. The flow rates of all the gases were regulated using mass-flow controllers (MKS, Type 1179A), which were calibrated for each individual gas mixture used in these experiments. The flow rates of the carrier gas (helium) were in the range of ~0.3-0.9 SLM and were much greater than the reactant gas flow rates. The movable injector (14 mm outer diameter) was also a stainless steel tube and its external surface was teflon lined.

Sampling system

A two stage differential pumping system was constructed (19) in order to sample a small fraction of the flow tube mixture into the ionization chamber of the photoelectron spectrometer. The experimental sampling system consists of two stainless steel chambers separated by thin discs with small holes in their centres. The hole sizes were selected, with the pumping system used, to allow a gradual decrease in pressure from the flow tube (~3 torr) down to 10^{-5} torr in the ionization chamber of the photoelectron spectrometer.

The flow tube (at 1.6-3.0 torr total pressure) was sampled through a hole of 2.5 mm diameter drilled in the centre of a teflon disc situated in Chamber 1 (1 in Fig.1) that is pumped by a SV 200 rotary pump. It is assumed that once the gas is sampled from the flow tube into the Chamber 1, no further reaction occurs. Chamber 2 (2 in Fig. 1) is pumped by a second rotary pump (D25B Leybold) to a pressure of approximately 10^{-1} torr. At the end of chamber 2 there is a second small hole co-axial with the first that is 5 mm diameter, drilled in the centre of a stainless steel disc leading into chamber 3 (3 in Fig.1). Chamber 3 is pumped by a third rotary pump (D25B Leybold) and is maintained at a pressure $\leq 10^{-2}$ torr. At the end of the third chamber there is a final stainless steel disc with a hole in the middle of 2 mm diameter (co-axial with the previous two holes).

Detection system

The end of the flow tube is situated in the ionization chamber of the photoelectron spectrometer (20, 21) and is aligned perpendicular to the radiation source, the helium discharge lamp. The photon beam was ~1.5 cm below the 2 mm hole of Chamber 3 (see Figure 1).

All photoelectron spectra were recorded using He Iα radiation (21.22 eV) on a single detector photoelectron spectrometer. Typical resolution under normal operating conditions was 25-30 meV as measured for the $(3p)^{-1}$ ionization of argon.

Experiments were carried out with the flow tube interfaced to the photoelectron spectrometer as shown in Figure 1 with the three sampling holes, diameters of 2.5, 5.0 and 2.0 mm, to evaluate the minimum detectable partial pressures in the flow-tube of Ar, DMS and Cl_2 from the measured intensities of their photoelectron bands. Also it was important to check the range of partial pressures of the gases in the flow tube over which the photoelectron signal, as measured with this set-up, was linear. The minimum detection limits for Ar, DMS and Cl_2 were estimated as $1x10^{11}$, $3.5x10^{11}$ and $4x10^{11}$ molecules cm^{-3} respectively. Also for these three gases the pressure range over which the photoelectron signal was linear with pressure in the flow tube was $1x10^{11}$ – $1.1x10^{14}$, $3.5x10^{11}$-$1.6x10^{13}$ and $4x10^{11}$- $1x10^{14}$ molecules cm^{-3} respectively.
(These experiments set the detection limit as a signal : noise ratio of 2 with an integration time of 1 sec.).

With this apparatus absolute photoionization cross-sections can be evaluated. This was achieved by recording PE spectra of a sample gas (such as DMS, Cl_2 and CH_3SCH_2Cl) at a known partial pressure in helium and PE spectra, recorded under the same conditions on the same day , of a known partial pressure of a second gas such as Ar in helium, for which the photoionization cross-section (σ) and angular distribution parameter (β) are known at the HeI photon energy. The results of these measurements will be presented in a separate paper (5).

The ionization energy (IE) scale of spectra recorded during kinetics experiments were calibrated using the first vertical ionization energy (VIE) of DMS (8.72 eV) (22) and either the lowest spin-orbit component of the first band of HCl (12.75 eV) (23) or the VIE of the second band of Cl_2 (14.43 eV) (24) when the HCl signal was either undetectable or out of scale.

Preparation of Reactant Gases

Each reagent, DMS (99+ %, Aldrich) or chlorine (99.9 %, Air Products) was mixed with He and stored in 6 L Pyrex bulbs. The mixtures (typically 10% Cl_2 in He and 1% DMS in He) were made by passing a gas of known pressure into an evacuated bulb and then filling the bulb to atmospheric pressure with He (BOC, CP grade). The gases were handled within a Pyrex manifold, with pressures being measured by 10, 100 and 1000 torr capacitance manometers (MKS). The freeze-pump-thaw method was used to purify DMS and chlorine. The He carrier gas was flowed through two molecular sieves to ensure removal of water, CO_2 and hydrocarbon impurities before entering the flow tube.

Results

Initial Survey Spectra

Although qualitative studies of the products of reaction (1) observed as a function of time have been made on another photoelectron spectrometer, and the results will be reported separately (5), it is useful to present survey spectra obtained with the spectrometer used in this work. In these survey experiments the initial concentrations of DMS and Cl_2 were kept constant and were approximately the same. The distance of the central injector from the sampling hole between Chambers 1 and 2 was changed in the range 0-35 cm and photoelectron spectra were recorded at each mixing distance. Some representative results are shown in Figure 2. Inspection of Figure 2 indicates that the first bands of DMS (vertical ionization energy (VIE) 8.72 eV) and Cl_2 (VIE 11.65 eV)decrease with reaction time whereas the bands associated with the products, HCl (VIE 12.75eV)

and CH_3SCH_2Cl (VIE 9.18 eV), increase with reaction time. Also, observed are bands associated with a long-lived reaction intermediate at 9.69 and 10.62 eV vertical ionization energy. The bands associated with the reaction intermediate were found in this and other studies to maximize and start to decrease before the product bands reach maximum intensity, and were assigned on the basis of photoelectron and infrared spectroscopic evidence to the intermediate $(CH_3)_2SCl_2$ (5).

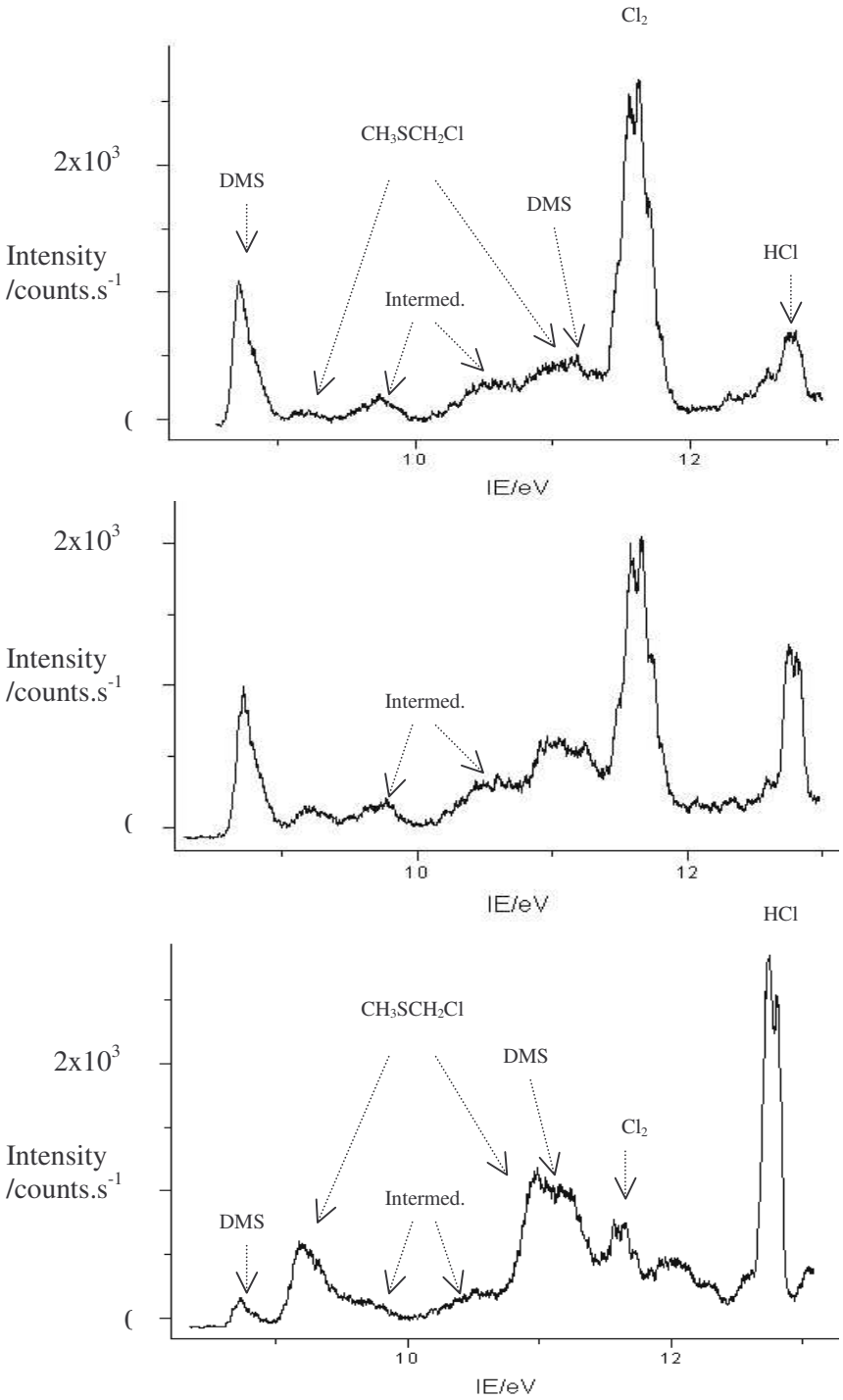

Figure 2. Spectra recorded at different mixing distances for the Cl_2 + DMS reaction. (a- 6 cm mixing distance, b -13 cm mixing distance, c- 25 cm mixing distance). It can be seen that the bands of DMS (first band at 8.72 eV) and Cl_2 (first band at 11.65 eV) decrease and the bands of CH_3SCH_2Cl (bands at 9.18 and 10.97 eV) and HCl (first band at 12.75 eV VIE) increase with mixing distance (reaction time) in the flow-tube. The initial partial pressures of DMS and Cl_2 in this experiment were approximately the same. The mixing distances shown in the caption are the distances of the movable injector in Chamber 1 above the small hole (2.5mm diam.) between Chamber 1 and Chamber 2 (see Fig.1). Bands associated with a reaction intermediate are labelled as 'Intermed.' .

Rate constant measurement

Reaction (1) was studied with [Cl_2] in excess over [DMS] at two different pressures, 1.6 and 3.0 torr. Flow velocities in the flow tube were approximately 4 ms^{-1} at 1.6 torr and 8 ms^{-1} at 3.0 torr. Helium was used as the carrier gas. In order to measure the rate constant of reaction (1), the most intense band of DMS observed at 8.72 eV VIE was used to monitor the change in DMS concentration after the addition of Cl_2 as a function of the mixing distance. In a typical experiment, DMS mixed in helium was allowed to pass through the flow-tube for about 30 minutes before the addition of Cl_2 in helium since DMS is relatively viscous and it was essential to reach stable conditions where a constant PE signal of DMS was obtained. Cl_2 was then added and the intensity of DMS was seen to drop. The helium carrier flow was reduced to maintain the fixed pressure in the flow tube. The injector was repositioned at a different mixing distance and the experiment repeated. The pseudo-first order rate constant at a known concentration of Cl_2 is given by the gradient of the plot of $\ln\left(\frac{[DMS]_0}{[DMS]_t}\right)$ against the contact time for different positions of the injector. Examples of the pseudo-first order plots are shown in Figure 3.

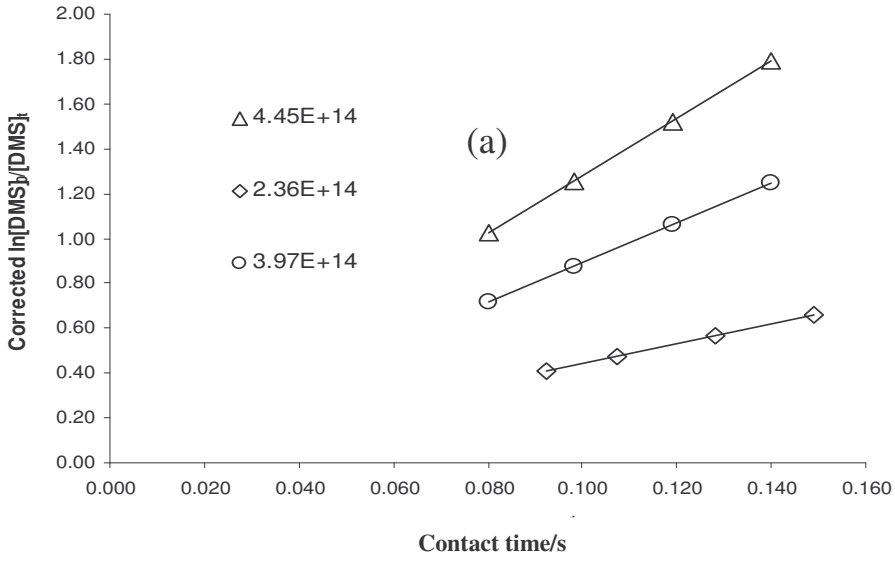

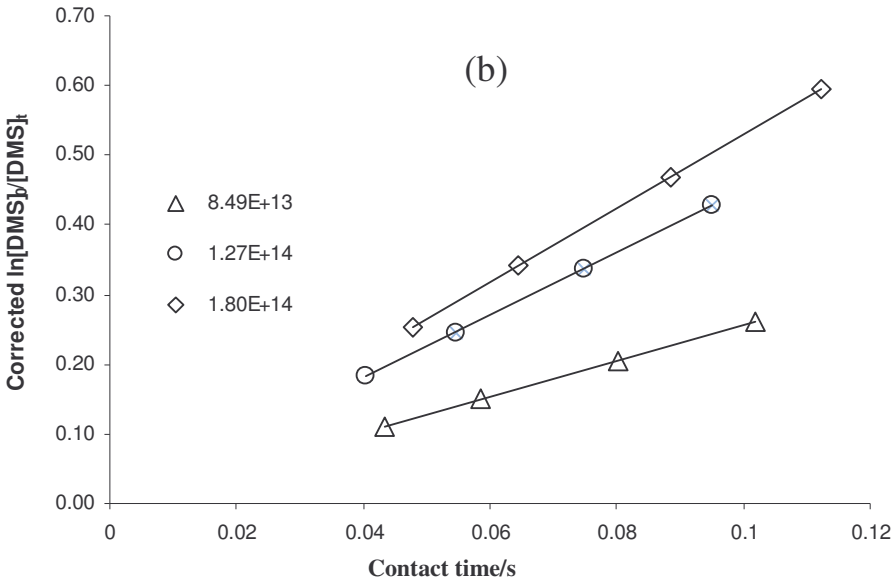

Figure 3. Typical pseudo-first order plots for reaction (1) at (a) 1.6 and (b) 3.0 torr respectively obtained from DMS decay kinetics in excess of Cl_2
(The values listed on each graph are the concentrations (molecules/cm^3) of Cl_2 used in each experiment). Each point has been corrected for wall losses (see text).

Wall losses were reduced by using an internal teflon coating in the flow-tube.
The wall loss rate constant, k_{wall}, was esumated by introducing DMS through the injector in the absence of chlorine at different mixing points above the 2.5mm sampling hole at the end of the flow-tube. In this way the contact time of DMS with the walls of the flow-tube could be changed and an estimate of the wall loss rate constant, k_w, could be made by plotting $\ln\left(\frac{[DMS]_0}{[DMS]_{t'}}\right)$ as a function of contact time (where $[DMS]_0$ is the concentration of DMS at zero contact time and $[DMS]_{t'}$ is the concentration of DMS at time t after the wall loss). It was found that the measured wall loss rate constant was very small, $k_{wall} \cong 0$, suggesting that heterogeneous losses were much smaller than the homogeneous losses. For each point in Figures 3(a) and (b), $\ln\left(\frac{[DMS]_0}{[DMS]_t}\right)$ has been corrected for this effect. Corrections were also made to the pseudo-first order rate constants for axial and radial diffusion using the method described by Keyser (25) with estimated values of the diffusion coefficient of DMS in helium at 1.6 torr of 164.6 cm^2s^{-1} and at 3.0 torr of 91.1 cm^2s^{-1}. These corrections gave rise to a correction in the pseudo-first order rate constant of less than 20% with the axial diffusion correction being an order of magnitude larger than the radial diffusion correction.

Plotting the corrected pseudo-first order rate constants against the molecular chlorine concentration yields the second order rate constant. The results obtained are (3.39±0.52) x 10^{-14} cm^3 $molecule^{-1}s^{-1}$ at 1.6 torr, Figure 4, and (3.41±0.70) x 10^{-14} cm^3 $molecule^{-1}s^{-1}$ at 3.0 torr, Figure 5, where the errors quoted are the statistical standard errors of the slopes (both values were determined at a temperature of (294±2) K).

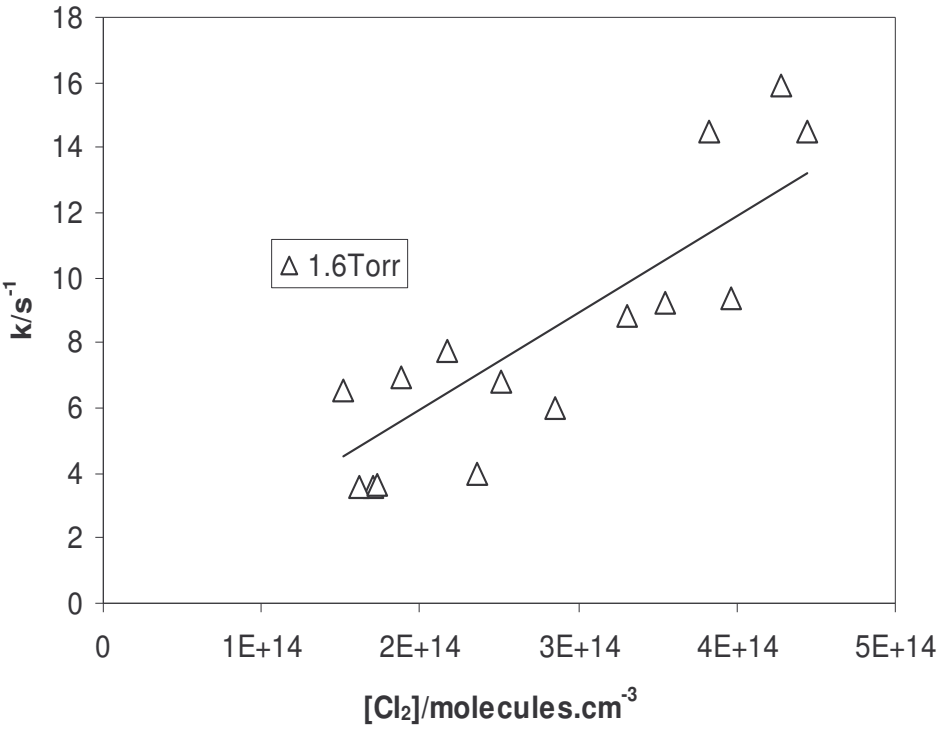

Figure 4: Second-order plot for the reaction of Cl_2 with DMS at a total pressure of 1.6 torr

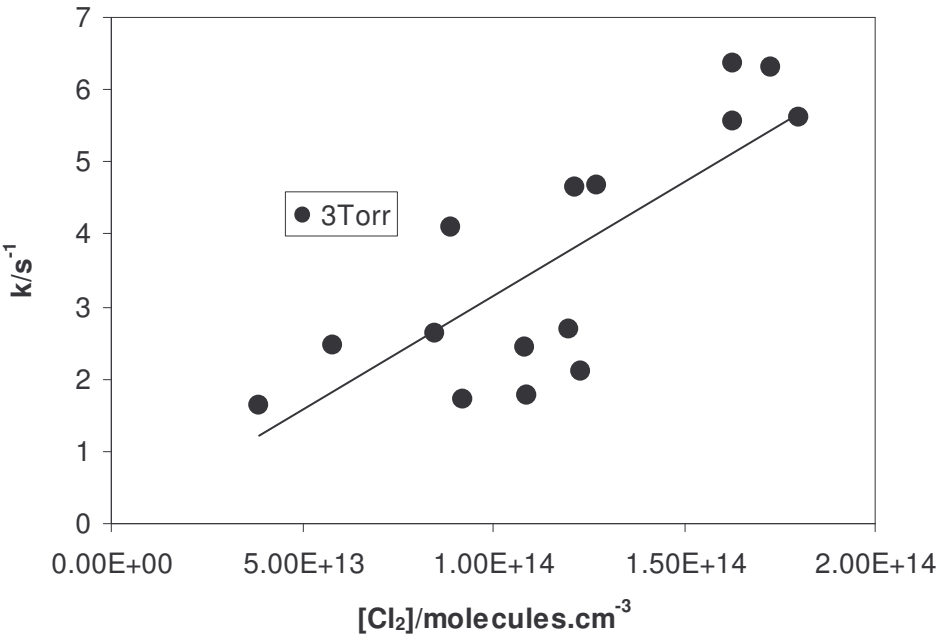

Figure 5: Second-order plot for the reaction of Cl_2 with DMS at a total pressure of 3 torr

A comparison of the results obtained at 1.6 and 3.0 torr is given in Figure 6. Overall the agreement between the two data sets is good, although an insufficient pressure range has been studied to estimate the pressure dependence fully. The values obtained for the second order rate constant at the two pressures are in good agreement with each other and it is reassuring that they are less than the upper limit value estimated by Butkovskaya et al.(17) of $8x10^{-14}$ $cm^3molecule^{-1}s^{-1}$ by discharge-flow electron impact mass spectrometry.

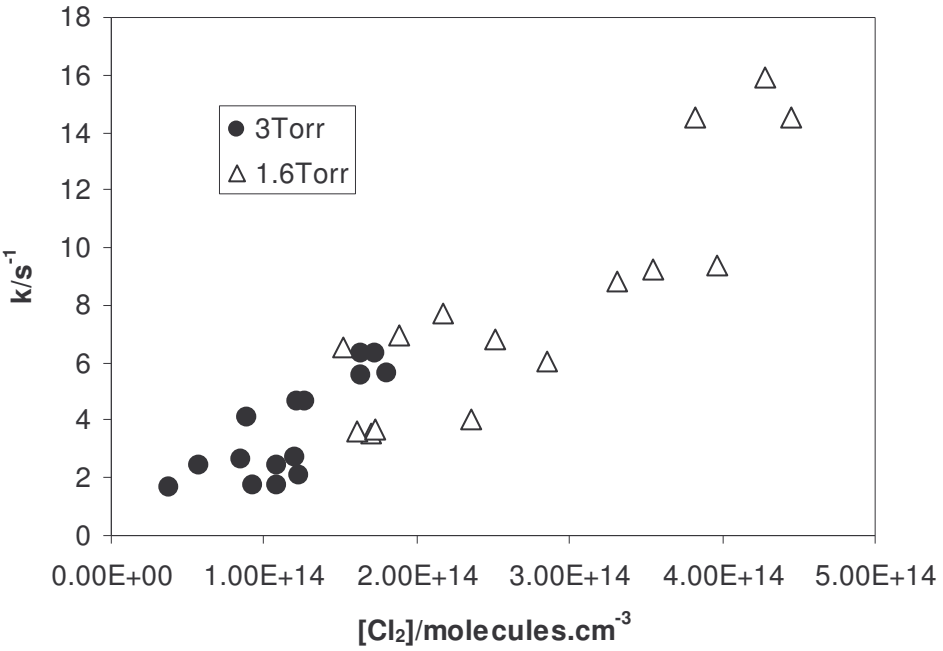

Figure 6. Combined second-order plots for the reaction of Cl_2 with DMS at a total pressure of 1.6 (open triangles) and 3.0 torr (filled circles)

Ab initio calculations

In order to investigate the mechanism of reaction (1), *ab initio* calculations have been carried out at the MP2 level using aug-cc-pVDZ (aVDZ) basis sets (26) with the GAUSSIAN03 programme (27). A search was made for minimum energy structures and transition states which are inter-connected on the potential energy surface between the reagents (Cl_2 and DMS) and the products (CH_3SCH_2Cl and HCl). Then for the minimum energy structures and transition states located at the MP2/aug-cc-pVDZ level, fixed point CCSD(T) calculations were performed to provide improved values of the total energies. The MOLPRO programme (28) was used for the CCSD(T) calculations. For all these CCSD(T) calculations, the T_1 diagnostic was acceptably small. In this procedure, the MP2 calculations include some dynamic electron correlation and the CCSD(T) calculations include higher order dynamic electron correlation.

Transition states were characterised via harmonic frequency analysis and connected to minimum energy structures through IRC (intrinsic reaction co-ordinate) calculations. The stationary points located on the potential energy surface are represented in Figure 7 where the computed energies of the stationary points obtained are shown as bold horizontal lines and the transition states are labelled TSn. As expected, the reactant-type intermediate DMS:Cl_2 and product-type intermediate CH_3SCH_2Cl:HCl were located as minimum energy structures . However, apart from the reactants and products, nine other minimum energy structures were located on the potential surface (see Figure 7), most notably a reaction intermediate $(CH_3)_2SCl_2$ (see Figure 8). In separate experiments (5), it was found that the photoelectron spectrum obtained for a reaction intermediate from reaction (1), bands at 9.69 and 10.62 eV in Figure 2 are part of this spectrum, could not be assigned to reactant or product-type intermediates, DMS:Cl_2 or CH_3SCH_2Cl:HCl, but could be assigned to $(CH_3)_2SCl_2$. There is also infrared evidence to support this conclusion (5). Computed minimum energy structures of the reactant intermediate (DMS:Cl_2, C_s), the intermediate ($(CH_3)_2SCl_2$) and the product intermediate (CH_3SCH_2Cl:HCl trans) are shown in Figure 8 and the computed structures of the transition states are shown in Figure 9.

Based on the schematic potential energy diagram shown in Figure 7, the reaction proceeds from the reactants, DMS and Cl_2, to a reactant-type intermediate DMS:Cl_2 then to a structure of the type $(CH_3)_2SCl$:Cl. It then passes over a transition state (TS1) to $(CH_3)_2SCl_2$, the intermediate associated with the photoelectron bands at 9.69 and 10.62 eV in Figure 2. This then decomposes via TS2, which is lower than TS1, to the products via a product-type intermediate. There is also a route which by-passes the $(CH_3)_2SCl_2$ intermediate via TS3 but this is higher in energy than TS1. Figure 7 indicates that the rate determining step of reaction (1) is passage over the TS1. This has an energy relative to the reactants of + 4.5 kcal.mol^{-1}($\Delta H^{\#}$ = 4.89 kcal.mol^{-1}, $\Delta S^{\#}$ = -37.8 cal.K^{-1}mol^{-1}). Use of these values for $\Delta H^{\#}$ and $\Delta S^{\#}$ with the standard transition state expression gives 1x10^{-20} cm^3 molecule^{-1} s^{-1} for the rate constant, clearly much lower than the experimentally measured rate constant of (3.4 ± 0.7) x10^{-14} cm^3 molecule^{-1} s^{-1}. This indicates that the energy of TS1 relative to the reactants is too high (probably by ≈1-2 kcal.mol^{-1}) and the computed entropy change from the reactants to TS1 is too negative. This almost certainly arises because a modest basis set has been used in the calculations performed in this work. Improved calculations would involve using a larger basis set. These should lead to improved values of $\Delta H^{\#}$ and $\Delta S^{\#}$ from the reagents to the TS1.

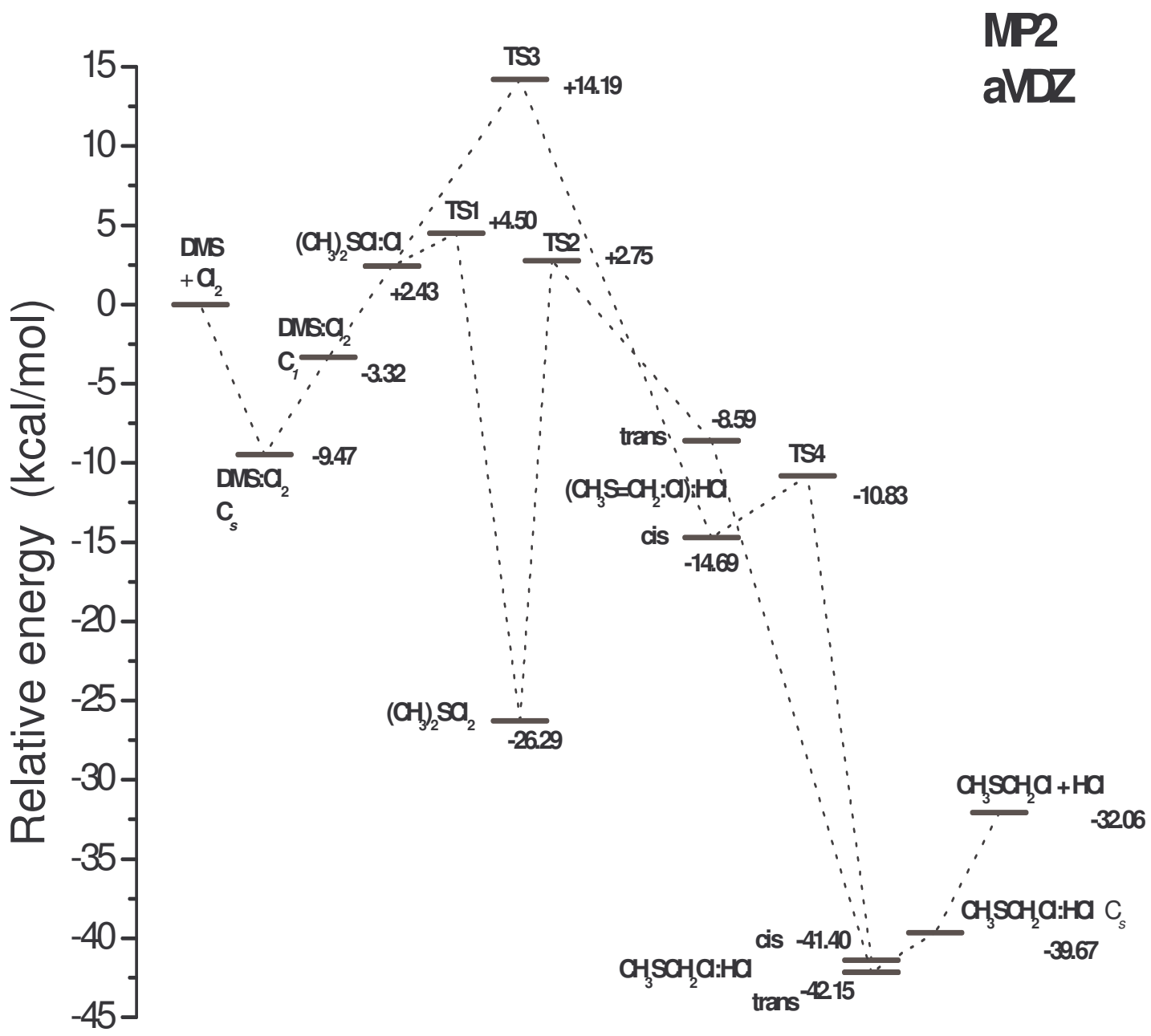

Figure 7 Relative electronic energy diagram for reaction (1). Minimum energy structures and transition states were located at the MP2/ aug-cc-pVDZ level. Then fixed point CCSD(T) calculations were performed to provide improved values of the total energies.

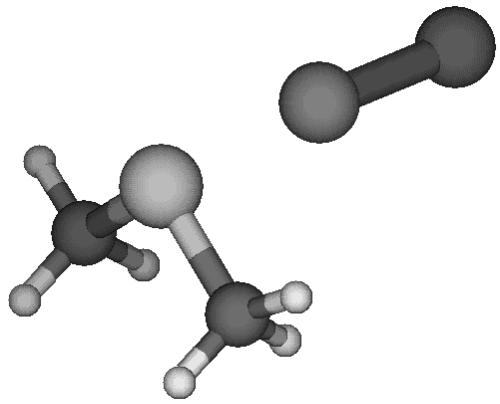

DMS:Cl_2 C_s

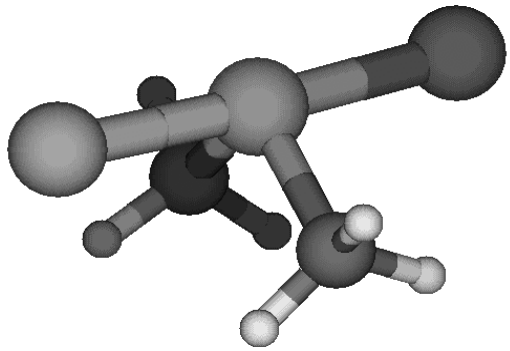

$(CH_3)_2SCl_2$

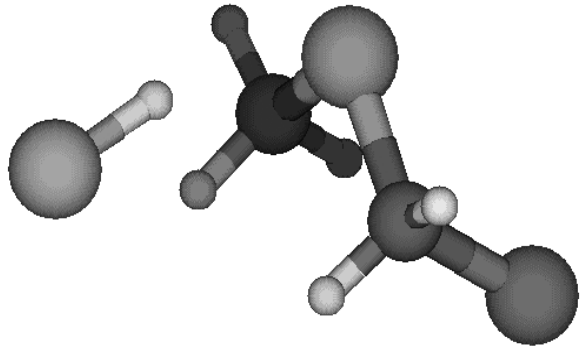

CH_3SCH_2Cl:HCl trans

Figure 8:
Computed minimum energy structures of the reactant-intermediate (DMS:Cl_2, C_s), the intermediate $(CH_3)_2SCl_2$, and the product-intermediate CH_3SCH_2Cl:HCl trans.

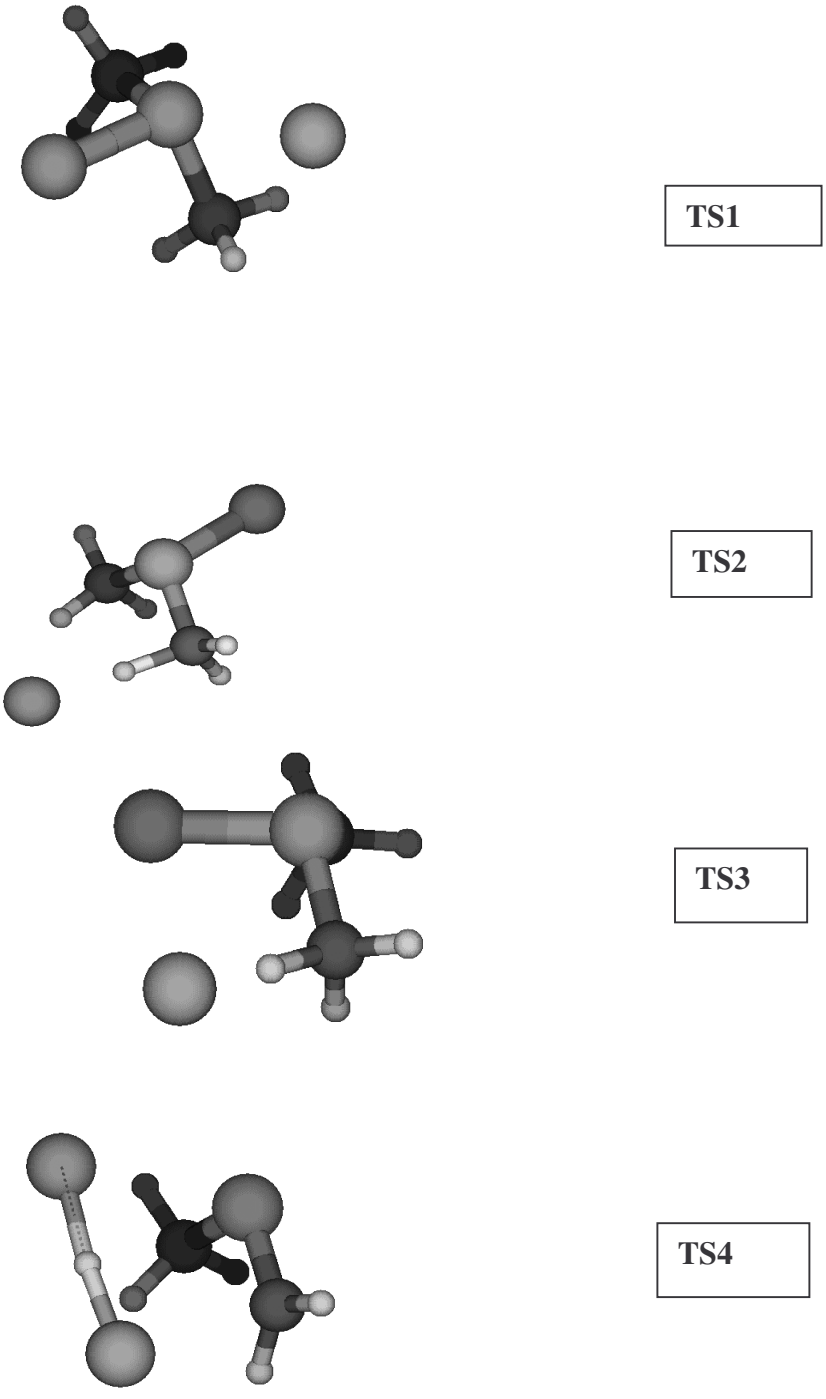

Figure 9

Transition states located on the potential surface of reaction (1) (see text and Figure 7).

Discussion

It is interesting to compare reaction (1) with the reaction between Cl and DMS, reaction (2). Both reactions involve formation of a complex, $(CH_3)_2SCl_2$ in the case of reaction (1) and $(CH_3)_2SCl$ in the case of reaction (2). The $(CH_3)_2SCl$ intermediate formed in reaction (2) has been detected by electron impact mass spectrometry (12), ultraviolet-visible absorption spectroscopy (15) and cavity-ring down laser spectroscopy (14) whereas the $(CH_3)_2SCl_2$ intermediate formed in reaction (2) has been observed in this work by photoelectron spectroscopy. A comparison of the computed molecular structures and geometrical parameters for these two complexes is made in Figure 10. In this figure, the parameters for the $(CH_3)_2SCl$ complex are taken from reference (16), where they were computed at the UMP2/DZP level, and the parameters for $(CH_3)_2SCl_2$ were computed in this work at the MP2/aug-cc-pVDZ level. These structures are surprisingly similar with the C-S-Cl angle equal to 91.9° in both cases. The Cl-S distance is longer and the C-S distance shorter in $(CH_3)_2SCl$ than in $(CH_3)_2SCl_2$ (see Figure 10). SCl_4 is also expected to have a very similar geometry with a pseudo trigonal-bipyramidal co-ordination geometry at the S atom. The Cl-S-Cl bond angle has been computed to be 169.7° for the axial Cl-S-Cl unit (29).

Reaction (2) is much faster than reaction (1) with the most recent measurement of the rate constant for this reaction being made by cavity-ring-down spectroscopy (14), with a rate constant at atmospheric pressure being obtained as $k_2 = (3.6 \pm 0.2) \times 10^{-10}$ cm^3 molecule^{-1} s^{-1}. The low pressure limit value is $(6.9 \pm 1.3) \times 10^{-11}$ cm^3 molecule^{-1} s^{-1} (12,13). Reaction (2) proceeds by two channels, (2a) the hydrogen abstraction channel, which is pressure independent, and (2b) the addition channel which is pressure dependent.

Stickel et al.(13), in a study of reaction (2) using time-resolved detection of Cl atoms, reported that the branching ratio of reaction (2a) approaches unity with decreasing total pressure and k_2 increases with pressure. Both reactions (2a) and (2b) are expected to have large rate constants, as they proceed without a barrier, whereas reaction 2c, decomposition of $(CH_3)_2SCl$ to CH_3 and CH_3SCl, is very slow because it has a high activation energy barrier of ≈18 kcal.mol^{-1} (16).

Reaction (1), unlike reaction (2), has only one pathway which can be written as:-

$$Cl_2 + CH_3SCH_3 + M \rightarrow (CH_3)_2SCl_2 + M \quad \text{----------} \quad (1a)$$

$$(CH_3)_2SCl_2 \rightarrow CH_3SCH_2Cl + HCl \quad \text{----------} \quad (1b)$$

Clearly it would be valuable to establish the pressure dependence of k_2, and the value of k_2 at atmospheric pressure will be of particular importance in atmospheric modelling calculations. In view of the relative values of k_1 and k_2, reaction (1) will not be important in the atmosphere during the day, when photolysis of Cl_2 to Cl will occur, but it will be important at night when conversion of DMS to CH_3SCH_2Cl will take place via reaction (1), as discussed in the next section.

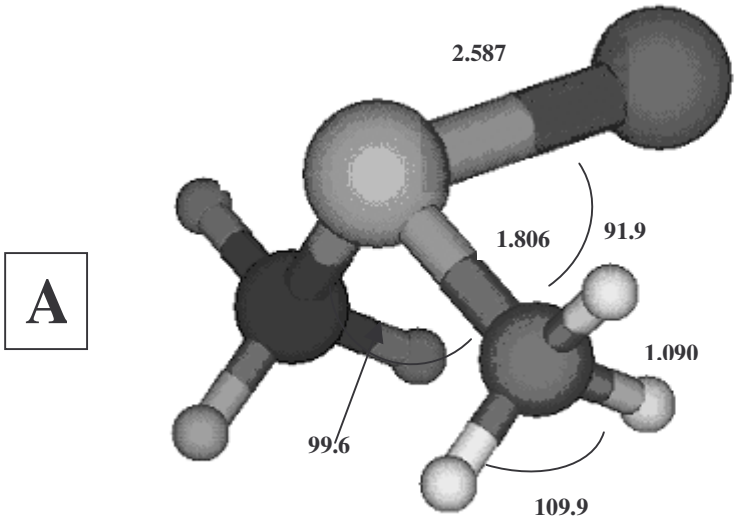

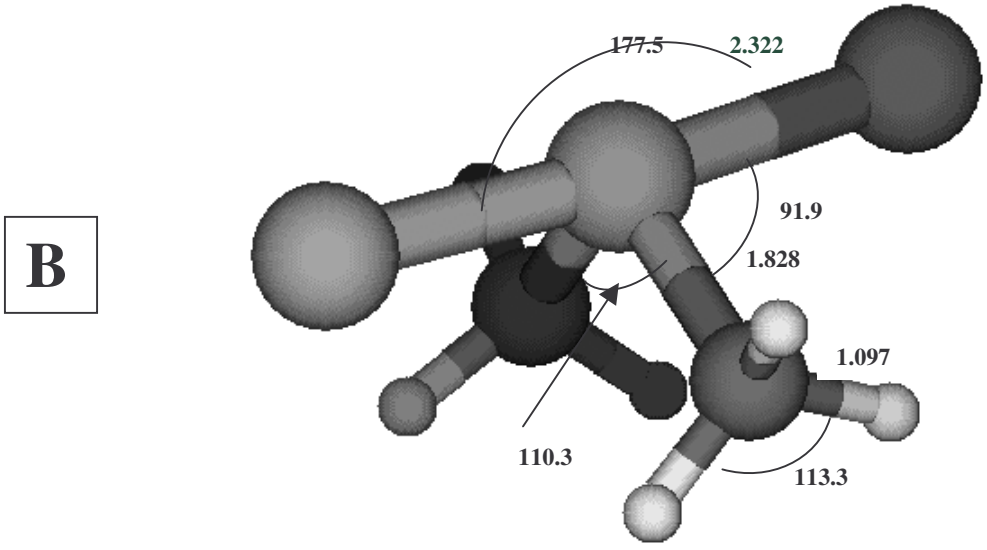

Figure 10
Computed structures for (A) the $(CH_3)_2SCl$ and (B) the $(CH_3)_2SCl_2$ intermediates. The $(CH_3)_2SCl$ structure was taken from ref. (16) computed at the UMP2/DZP level and the $(CH_3)_2SCl_2$ structure was computed in this work at the MP2/aug-cc-pVDZ level.

Atmospheric Implications

The oxidation of DMS has been highlighted by Charlson and co-workers (30) as being a potentially important natural pathway for the generation of cloud condensation nuclei (CCN), and could provide a key negative feedback to the earth's radiative balance. Crucial to the assessment of this 'CLAW' hypothesis is an understanding of factors that control the flux of DMS from the oceans to the atmosphere; these include sea surface temperature, surface wind speed, CO_2 levels, nutrient levels *etc*, some or all of which may change significantly in the wake of climate change. However, once in the atmosphere, in order for DMS to affect aerosol loading the rate of its oxidation and subsequent conversion to SO_2 and then H_2SO_4 is crucial. There have been many field and laboratory studies in the last decade (e.g. 31-34) and yet there are still considerable uncertainties concerning the oxidation of DMS (35). However, it appears from field studies in particular that DMS oxidation in the atmosphere is more rapid than can be accounted for using existing models, or more correctly, the production of SO_2 (assumed from DMS) is more rapid than expected. The dominant oxidant for DMS is thought to be the OH radical, and although there is evidence that the NO_3 radical can be an important oxidant at night in coastal areas (36), its significance in the open ocean is thought to be very small. Halogen chemistry has recently been considered as a possibility to account for the increased oxidation rate (35), and may well be part of the puzzle. The reactive halogen species involved will include Cl atoms, BrO radicals (37) and possibly IO radicals (38).

This present work has shown that the interaction between Cl_2 and DMS is not very slow, and that it produces molecular products CH_3SCH_2Cl and HCl. There are field observations that Cl_2 levels can reach 150 ppt at night. If it is assumed that the average level of Cl_2 at night is 50 ppt, then the lifetime of DMS at night with respect to reaction (1) is around 6 hours. If it is assumed that DMS levels are on average 50 ppt at night (field measurements suggest that this is perfectly reasonable in the southern ocean for example) and that the DMS and Cl_2 levels are being replenished at night to maintain these levels, over a six hour period, around 40 ppt of CH_3SCH_2Cl would be generated, assuming that CH_3SCH_2Cl simply builds up at night. In the morning, photolysis of Cl_2 will be rapid and reaction (1) will be ineffective as Cl_2 levels fall rapidly, but the CH_3SCH_2Cl, which has built up during the night, can either react with OH or be photolysed. The fate of CH_3SCH_2Cl will be discussed more fully in forthcoming papers; however, work from this laboratory suggests that photolysis to yield CH_3S and CH_2Cl will be quite rapid, with a CH_3SCH_2Cl lifetime of several hours. CH_3S is known to undergo rapid oxidation to CH_3SO_2 *via* reaction with NO_2 or O_3 and CH_3SO_2 is known to undergo thermal decomposition to yield SO_2 and CH_3. Therefore, the night-time interaction between Cl_2 and DMS may well provide a mechanism to speed up SO_2 production in the day and go some way to explain the discrepancy between DMS decay rates and SO_2 production rates during the day. If the levels of Cl_2 observed by Spicer and co-workers (11) are representative of the open ocean, then reaction (1) could play an important role in DMS oxidation and the coupling between halogens and DMS cannot be ignored in climate studies.

Conclusions

A flow-tube has been interfaced to a photoelectron spectrometer chemistry for the first time in order to measure rate constants of reactions of importance in atmospheric chemistry. The reaction between Cl_2 and DMS was the first reaction to be studied in this way and its rate constant was measured at 1.6 and 3.0 torr at room temperature, (294±2) K, returning a value of $k_1 = (3.4 \pm 0.7) \times 10^{-14}$ cm^3 $molecule^{-1}$ s^{-1}.
Photoelectron spectra recorded as a function of reaction time and supporting molecular orbital calculations showed that the reaction proceeds through an intermediate, $(CH_3)_2SCl_2$, which has a lifetime of ≈30 ms under the conditions used, with subsequent production of CH_3SCH_2Cl and HCl. The atmospheric implications of these results have been briefly discussed.

Acknowledgements

The authors gratefully acknowledge support of this work from NERC *via* a COSMAS grant, which also supported M.V.G with a postdoctoral fellowship. G.L. was supported by a postgraduate studentship from the EU Reactive Intermediates Network. The authors also gratefully acknowledge advice from and discussions with Dr C.E. Canosa-Mas and Professor R.P.Wayne of Oxford University and Dr. E.P.F. Lee of Southampton University. The Biogeochemistry Research Centre at Bristol University is a joint initiative between the School of Chemistry and the Departments of Earth Science and Geography.

References

1. J.M.Dyke, A.R.Ellis, N.Jonathan and A.Morris
J.C.S Faraday II 81, 1985, 1573

2. D.Wang, X.Qian and J.Peng
Chem Phys Letts 258, 1996, 149

3. X.Cao, X.Qian, C.Qiao and D.Wang
Chem Phys Letts 299, 1999, 322

4. (a) D.Wang and X.Qian J.Elect Spec Rel Phen 83, 1997, 41
(b) D.X.Wang, S.Li, D.Wang and Y.Li J.Elec Spec Rel Phen 70, 1994, 173

5. J.M.Dyke, M.V.Ghosh, M.Goubet, G.Levita, K.Miqueu, J.S.Ogden,
and D.E.Shallcross unpublished work

6. C.F.Cullis and M.M.Hirschler Atmos. Environ. 14, 1980, 1263

7. H.Rodhe and I.Isaksen J.Geophys. Res. 85, 1980, 7401

8. T.S.Bates, B.K.Lamb, A.Guenther, J.Dignon and R.E.Stoiber
J.Atmos.Chem 14, 1992, 315

9. H.Berresheim, P.H.Wine, and D.D.Davis in
Composition, Chemistry and Climate of the Atmosphere
van Nostrand Reinhold, New York 1995, p251

10. Y.Sadanaga, J.Hirokawa and H.Akimoto
Geophysical Research Letters 28, 2001, 4433

11. C.W.Spicer, E.G.Chapman, B.J.Finlayson-Pitts, R.A.Platridge,
J.M.Hubbe, D.J.Fast and C.M.Berkowitz
Nature 394, 1998, 353

12. Y.Diaz-de-Mera, A. Aranda, D. Rodrigues, R.Lopez, B. Cabanas and E. Martinez
J.Phys Chem A 106, 2002, 8627

13. R.E. Stickel, J.M.Nicovich, S. Wang, Z. Zhao and P.H. Wine
J.Phys Chem 96, 1992, 9875

14. S.Enami, Y.Nakano, S.Hashimoto, M.Kawasaki, S.Aloisio and J.S.Francisco
J.Phys Chem A 108, 2004, 7785

15. S.P. Urbanski and P.H. Wine
J.Phys Chem A103, 1999, 10935

16. S.M. Resende and W.B. Almeida
J.Phys Chem A 101, 1997, 9738

17. N.I. Butkovskaya, G.Poulet and G.LeBras
J.Phys Chem 99, 1995, 4536

18. C. Howard, J. Phys.Chem, Vol.83, 1979, 3

19. D.J. Hucknall and A. Morris, Vacuum Technology, Calculations in Chemistry, Royal Society of Chemistry, Cambridge UK 2003

20. J.M.Dyke, A.Morris and N.Jonathan Int. Rev Phys Chem 2, 1982, 3

21. J.M.Dyke, N.Jonathan and A.Morris
Electron Spectroscopy Vol 3,1979, 189 Academic Press London

22. K. Kimura et al, Handbook of He I photoelectron spectra
Japan Scientific Societies Press, Tokyo, Halsted Press 1981

23. D.W.Turner, C.Baker, A.D.Baker, and C.R.Brundle
Molecular Photoelectron Spectroscopy Wiley-Interscience, London, 1970

24. A.B. Cornford, D.C. Frost, C.A. McDowell, J.L. Ragle, and I.A. Stenhouse
J.Chem. Phys. 54, 1971, 2651

25. L.F.Keyser, J. Phys Chem 88,1984, 4750

26. (a) R.A. Kendall, T.H. Dunning, Jr. and R.J. Harrison,
J.Chem Phys 96, 6796 (1992).
(b) D.E. Woon and T.H. Dunning, Jr.
J. Chem. Phys. 98, 1358 (1993).
(c) T.H. Dunning, Jr.
J. Chem. Phys. 90,1007 (1989).

27. Gaussian 03, Revision B.01, M. J. Frisch, G. W. Trucks, H. B. Schlegel, G. E. Scuseria, M. A. Robb, J. R. Cheeseman, J. A. Montgomery, Jr., T. Vreven, K. N. Kudin, J. C. Burant, J. M. Millam, S. S. Iyengar, J. Tomasi, V. Barone, B. Mennucci, M. Cossi, G. Scalmani, N. Rega, G. A. Petersson, H. Nakatsuji, M. Hada, M. Ehara, K. Toyota, R. Fukuda, J. Hasegawa, M. Ishida, T. Nakajima, Y. Honda, O. Kitao, H. Nakai, M. Klene, X. Li, J. E. Knox, H. P. Hratchian, J. B. Cross, C. Adamo, J. Jaramillo, R. Gomperts, R. E. Stratmann, O. Yazyev, A. J. Austin, R. Cammi, C. Pomelli, J. W. Ochterski, P. Y. Ayala, K. Morokuma, G. A.

Voth, P. Salvador, J. J. Dannenberg, V. G. Zakrzewski, S. Dapprich, A. D. Daniels, M. C. Strain, O. Farkas, D. K. Malick, A. D. Rabuck, K. Raghavachari, J. B. Foresman, J. V. Ortiz, Q. Cui, A. G. Baboul, S. Clifford, J. Cioslowski, B. B. Stefanov, G. Liu, A. Liashenko, P. Piskorz, I. Komaromi, R. L. Martin, D. J. Fox, T. Keith, M. A. Al-Laham, C. Y. Peng, A. Nanayakkara, M. Challacombe, P. M. W. Gill, B. Johnson, W. Chen, M. W. Wong, C. Gonzalez, and J. A. Pople, Gaussian, Inc., Pittsburgh PA, 2003.

28. MOLPRO is a package of ab initio programs written by H.-J. Werner and P.J. Knowles; with contributions from J. Allmf, R. D. Amos, A.Berning, D.L. Cooper, M. J. O. Deegan, A. J. Dobbyn, F. Eckert, S. T. Elbert, C. Hampel, R. Lindh, A. W. Lloyd, W. Meyer, A. Nicklass, K. Peterson, R. Pitzer, A. J. Stone, P. R. Taylor, M. E. Mura, P. Pulay, M. Schutz, H. Stoll and T. Thorsteinsson.

29. Y.Drozdova, R.Steudel, W.Koch, K.Miaskiewicz and I.A.Topol Chem. Eur. J. 6, 1999, 1936

30. R.J. Charlson,J.E. Lovelock, M.O. Andreae and S.G. Warren Nature (London), 326,1987, 655.

31. W.J.Bruyn,, Harvey, M., Cainey, J.M. and Saltzman, E.S. J. Atmos. Chem., 41, 2002,189

32. G.Chen, D.D.Davis, P.Kasibhatla, B.R.Bandy, D.C.Thornton, B.J.Huebert A.D.Clarke, and B.W.Blomquist, J. Atmos. Chem., 37, 2000,137

33. J. Sciare, E.Baboukas, and N.Mihalopoulos J. Atmos. Chem., 39, 2001, 281.

34. G.Knight, and J.N.Crowley Phys. Chem. Chem. Phys., 3, 2001,393.

35. D.D.Lucas, and R.G.Prinn J. Geophys. Res., 107, 2002, 10.1029/2001 JD000843

36. H.Bardouki, H.Berresheim, J.Sciare, G.Kouvarakis, J.Schneider, and N. Mihalopoulos Atmos. Chem. Phys., 3, 2003, 1871.

37. T. Ingham, D.Bauer, R.Sander, P.J.Crutzen, and J.N.Crowley J. Phys. Chem., 103,1999, 7199.

38. J.D.James, R.M.Harrison, N.H.Savage, A.G.Allen, J.L.Grenfell, B.J.Allan, J.M.C.Plane, C.N.Hewitt, B.Davison, and L.Robertson *J. Geophys. Res*., 105, 2000, 26,379.